High-Energy Runaway Electrons in the Oak Ridge Tokamak*

H. Knoepfel† and S. J. Zweben‡
Oak Ridge National Laboratory, Oak Ridge, Tennessee 37830
(Received 16 June 1975)

Measurement of hard x-rays produced in normal ORMAK discharges provides direct evidence that runaway electrons can be produced at early times and can be contained stably during the whole discharge time, thereby attaining energies of the order of 10 MeV. This class of high-energy runaway electrons complements and extends previous information on runaways in toroidal discharges and can have some distinct consequences on the operation of future tokamak devices.

Relativistic runaway electrons in toroidal plasma devices have been studied consistently since the mid-fifties, first in connection with the plasma betatron experiments[1] and then in stellarators.[2] More recently, runaway electrons have been generated in tokamaks,[3] notably in ORMAK,[4] and some experimental[5] and, particularly, theoretical effort has been devoted to this problem in the past.[6] Most of this work centered on two different runaway regimes. In the first, which is obtained at low densities ($\bar{n}_e \lesssim 10^{13}$ cm^{-3}) and with a relatively poor preionization and/or high impurity content in the filling gas, electrons are accelerated into the runaway state at the very early discharge times and then carry an appreciable part of the total plasma current.[4] In the second, studied in detail on the ST device at Princeton University,[7] runaway electrons are formed continuously in the hot central part of a normal discharge and gradually build up a high-energy "runaway tail" in the electron distribution function. In this paper we present experimental evidence for a third group of runaway electrons that are characterized by (a) very high final energies (in the 10-MeV range); (b) being generated at early times (0.5–10 msec) and (c) on the outer magnetic surfaces ($r_c \approx 10$–20 cm); and (d) being stably contained during the whole discharge (up to 80 msec).

The experimental study concentrated mainly on the measurement and analysis of the very hard bremsstrahlung spectrum produced by the runaway electrons when hitting a thick target (the limiter). This information is compared and processed with the other data available from the ORMAK diagnostic system. The basic elements of our diagnostic system are two large (12.5 cm $\times$12.5 cm and 7.5 cm$\times$7.5 cm) NaI(Tl*) crystal detectors, each housed in a heavy but movable lead collimator. Because hard bremsstrahlung is strongly peaked in the forward direction,[8] the detectors look tangentially towards the target. The scintillation pulses are processed in a pile-up rejection system with a resolution of 100–200 nsec, and then stored in a multichannel analyzer relative to four selectable time intervals and also recorded photographically from different oscilloscopes. The (maximum) energy and corresponding intensity of the detected runaway electrons is found by matching the scintillation spectrum with ideal curves obtained by correcting the experimentally determined thick-target bremsstrahlung spectra[8] for absorption in the beam line, and then unfolding into the corresponding scintillation pulse-height spectra.

Measurements of bremsstrahlung spectra were made in connection with normal discharges in ORMAK.[9] The highest intensities and energies (reproducibly in the 7–14-MeV range) are found in the stable, low-density ($\bar{n}_e \approx 1.2\times10^{13}$ cm^{-3}), so-called type-B discharges, in which the runaway electrons are lost mainly towards the end of the discharge. In the higher-density, mildly magnetohydrodynamically unstable, type-A discharges, in which the runaway electrons are lost at the beginning, the intensity is much lower. The characteristic hard bremsstrahlung signature of all these discharges can be basically understood in terms of the runaway electrons intercepting the target as their orbits shift by $d_p + d_\gamma$ along the major radius R of the toroidal discharge chamber; here d_p is the shift of the whole plasma column with respect to the chamber and d_γ is the outward shift of the runaway orbits with respect to the plasma column. On top of the basic and smooth process we find that additional effects may in some circumstances enhance the loss of runaway electrons, as for example, increased centrifugal diffusion of runaway electrons in the scrape-off layers due to magnetic field ripple,[5] magnetohydrodynamic activity,[3,10] etc.

The orbit of an accelerated electron consists

of a fast gyration at the toroidal-field Larmor frequency about a guiding center that itself moves on a drift surface as the result of the movement along the helical field lines and the vertical drift; for runaway electrons the latter is determined principally by the curvature drift. The resulting outward shift d_γ of the drift surface with respect to the related magnetic surface with radius r_c (on which the runaway electron was born) is given approximately by[11] $d_\gamma \approx \rho_{L_p} r_c/R$, where $\rho_{L_p} = v_\parallel/\Omega_p$ is the poloidal-field (B_p) Larmor radius ($\Omega_p = eB_p/\gamma m_0 c$), γ is the relativistic energy factor [kinetic energy $W_R = m_0c^2(\gamma - 1)$], and $v_\parallel = \beta_\parallel c$ is the longitudinal electron velocity. For orbits located outside of most of the plasma current, i.e., $r_c \gtrsim 0.8 r_L$, we take $B_p = 21/cr_c$ and obtain $d_\gamma \approx r_c^2 I_A/2RI$, where $I_A = \beta_\parallel \gamma m_0 c^3/e = 17\beta_\parallel\gamma$ kA is the Alfvén current. Notice that for a 10-MeV ($\gamma = 21$) electron in ORMAK ($R = 80$ cm, $r_L = 23$ cm, $I = 100$ kA, $r_c/r_L = 0.8$) one finds typically $d_\gamma \approx 8$ cm; here r_L is the radius of the limiter that defines the largest poloidal extension of the discharge. Numerically computed trajectories for ORMAK type-B discharges show that a useful approximation for large shifts (of orbits touching the limiter, $d_\gamma + d_p + r_c = r_L$) and for $0.2 r_L \lesssim r_c \lesssim 0.85 r_L$ is $d_\gamma/r_L = 0.082 I_A/I + 0.053$. The orbit-shift model correctly predicts many properties of the measured high-energy runaway electrons, as for example the intensity increase, when the overall current starts to decay [see for example Fig. 1(b)]. In principle, it can provide the radial distribution of runaway energy, $\gamma(r_c)$, and density, $n_R(r_c)$, from the measured energy and intensity curves (as those given in Fig. 1), thus representing an interesting diagnostic method for probing the inner plasma regions; but the intrinsic uncertainty in the diagnostic method does not allow at present such a detailed quantitative evaluation.

Figure 2 shows the characteristic early-time evolution of the measured maximum runaway energy during a type-A discharge. The comparison

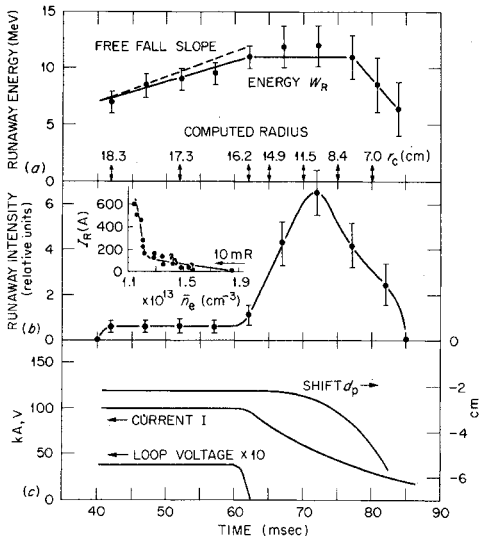

FIG. 1. Time evolution of the measured energy, intensity, and computed radius of runaway electrons that interact with the target in typical type-B discharges (7900 series). The variation of the total runaway intensity (as measured by the pulse analysis system for $E > 3$ MeV and expressed by the corresponding toroidal current I_R) versus the line-averaged electron density $\bar{n}_e$ is shown in the inset; the marked radiation level of 10 mR per shot is referred to the outside surface of the large ORMAK container.

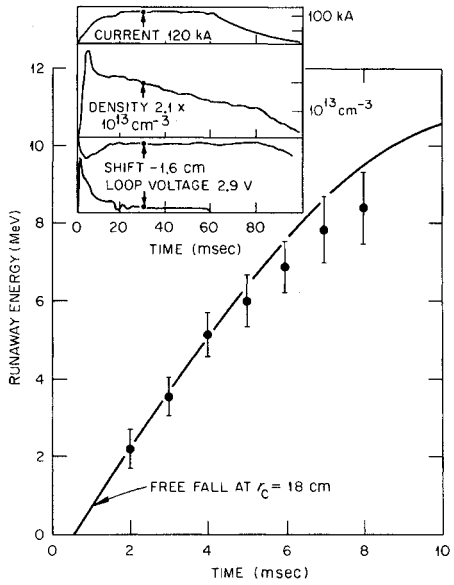

FIG. 2. Maximum energy of runaway electrons dumped at the target in representative ORMAK type-A discharges (6200 series) of which some typical parameters are given in the inset. Also shown is the free-fall curve describing the relativistic kinetic energy that a free electron, born at $t = 0.5$ msec and sitting on a magnetic surface with minor radius $r_c = 18$ cm, would gain in the locally applied electric field. The measured overall bremsstrahlung intensity is typically lower by a factor 50 with respect to that produced in a mean type-B discharge as described in Fig. 1.

with the free-fall curve[4] indicates that in these discharges the runaway electrons have been generated within 0.5 msec from the start of the discharge. Then they are accelerated as nearly free electrons for at least the first 4–5 msec and are gradually lost to the limiter during the first 10 msec. Once the early runaway electrons have been skinned off from the plasma surface, no hard bremsstrahlung is detected at later times in type-*A* discharges. This effect, as well as the orbit calculations, indicates that these early runaway electrons must have been generated at the outer plasma layers ($r_c \approx 19$–20 cm). The large initial inward shift of the whole plasma column in these discharges (see inset of Fig. 2) actually allows the orbit to be contained long enough for the electrons to gain the measured energy (otherwise they would hit the limiter earlier at energies below about 0.3 MeV as is the case for type-*B* discharges). The measured number of runaway electrons in these discharges (with filling pressures of around 0.25 mTorr hydrogen) is much larger than that expected from theoretical predictions,[12] unless one assumes a pronounced skin effect with strong local heating. More likely, however, the runaway electrons are produced in partially ionized gas, where, in fact, higher generation rates can be expected. The initial large voltage pulse applied to the discharge (see inset) enhances the runaway-electron production and acceleration at early times, particularly at the outer layers, where inductive effects are at a minimum.

The energy and intensity of runaway electrons that are lost to the target during type-*B* discharges are shown in Fig. 1. In these discharges the dominant part of early runaway electrons must have been generated from about 2 to 10 msec. The runaway electrons thus miss a fraction of the possible kinetic energy they could gain in the initial large voltage pulse. It can be estimated[12] that plasma conditions in ORMAK [$T_e \approx 100$–200 eV, $\bar{n}_e \approx (1-2)\times 10^{13}$ cm^{-3}] are favorable for the runaway electrons to be generated in about the mentioned time interval. Following this phase, there is generally a period during which runaway electron production is quenched because the electric field has decreased more than the temperature has increased. Finally, after about 30 msec a steady regime follows where, according to the same estimates, runaway electrons are formed mainly in the inner, hot (600–800 eV) regions.

The energy of the detected high-energy electrons for type-*B* discharges [Fig. 1(a)] increases for as long as the voltage is applied to the discharge, and only slightly less than indicated by the slope of the free-fall curve. This shows that when the runaway electrons have attained energies in the MeV range they move around the discharge practically as free electrons. Since electrons are only lost after about 40 msec, no direct information is available here concerning the acceleration process. From a detailed spectral analysis of the bremsstrahlung produced after the loop voltage ends, we conclude that each of the discharges used to plot Fig. 1 contains an average of $N_R = 10^{13}$ runaway electrons in the 9–12-MeV range (corresponding to a toroidal current of $I_R = N_R \beta_{\parallel} ce/2\pi R \approx 100$ A), where N_R is determined to within a factor of 3. In addition, there are less-intense energy components in the 4–9-MeV range, with a total number of runaway electrons of about the same order (10^{13}). The bremsstrahlung and the corresponding scintillation spectrum produced by these runaway electrons so predominate over the ones generated by lower-energy components that no quantitative information can be given for these discharges on the electron distribution below about 3 MeV.

The approximated radii r_c, determined from the idealized intersection condition of the shifted orbits ($d_p + d_\gamma + r_c \equiv r_L$), are indicated for some of the runaway components in Fig. 1(a). Within the limits of this simplified analysis, it follows that these runaways must have been formed predominantly at radii of about 9 to 18 cm. In the inset of Fig. 1(b) the runaway intensity (expressed in terms of the current I_R) in a series of type-*B* discharges with maximum runaway energies of around 10 MeV is plotted versus the line-average density $\bar{n}_e$ measured by the microwave interferometer at 10 msec from the start of the discharge. A sharp increase in the runaway intensity is obtained at densities below 1.24×10^{13} cm^{-3}. Though the figure may vary by $\pm 10\%$ in other experimental runs depending on different machine conditioning, this effect is typical for the runaway-electron production in ORMAK.

Thus the experimental results may be summarized by noting that for high-density (type-*A*) discharges the runaway electrons were born before 1 msec and had maximum energies consistent with a free-fall acceleration up to about 8 MeV (Fig. 2); for low-density (type-*B*) discharges the electrons are again accelerating at nearly free fall between 40 and 60 msec, with energies such thay they must have been born at $\lesssim 10$ msec (Fig. 1). The fact that for high densities the x rays are observed only at the beginning, and for

low densities only near the end, is explained by an orbit-shift model which indicates that the former were born nearer the plasma's outer edge. The total runaway intensity is generally increased as the density decreases, with a rapid rise below $\approx 10^{13}$ cm^{-3}, but for normal operation the discharge contains only on the order of 100 A of electrons with $E > 3$ MeV.

The group of high-energy runaway electrons described in this paper not only can influence some of the discharge characteristics, but has some practical consequences, particularly on the interpretation of experimental results. Because of the production of copious bremsstrahlung quanta in the most penetrating energy range of above 1 MeV, information on the hard x-ray spectrum is essential to evaluate the interference of backgound radiation on many diagnostic systems. In addition, neutron production by photoneutron reactions in the limiter material[8] (threshold in tungsten 6–7 MeV) or by electron-induced Coulomb dissociation of deuterium (threshold 2.2 MeV) can be of the same order of magnitude, or higher, than thermonuclear reactions in today's D-T plasmas with ion temperatures of 500 eV (typically 10^6–10^7 neutrons/msec for the very moderate runaway discharges illustrated in Fig. 1 with $\bar{n}_e \simeq 2\times10^{13}$ cm^{-3}). Since the drift surfaces of the high-energy runaway electrons are shifted substantially with respect to the magnetic surfaces, it would require specially designed divertors to dump them efficiently. This requirement could be important for the future generation of larger tokamak devices, in which the high-energy runaway-electron population should increase both in energy and in number. Our experimental results indicate that these runaway electrons can be controlled and reduced by various by means, i.e., shaping and reducing the initial voltage pulse, controlling the densities, and dumping the runaway electrons at early enough times by a convenient shift of the plasma column.

In conclusion, we would like to acknowledge the many direct and indirect contributions to this work by all the members of the ORMAK group, particularly by L. A. Berry, P. H. Edmonds, and M. Murakami; and also we want to thank J. F. Clarke for his stimulating support and D. A. Spong for his analysis of the runaway-electron orbits.

---

*Research sponsored by the U. S. Energy Research and Development Administration under contract with the Union Carbide Corporation.

†On leave from Laboratorio Gas Ionizzati (EURATOM–Comitato Nazionale per l'Energia Nulceare), Frascati, Italy.

‡Oak Ridge Associated Universities Graduate Participant from Cornell University, Ithaca, N. Y.

[1]For example, J. F. Linhart *et al.*, in *Proceedings of the CERN Symposium on Nuclear Accelerators, Geneva, 1959* (CERN Scientific Information Service, Geneva, 1959), p. 139.

[2]For example, E. B. Meservey and L. P. Goldberg, Phys. Fluids 4, 1307 (1961).

[3]V. S. Vlasenkov, V. M. Leonov, V. G. Merezhkin, and V. S. Mukhovatov, Nucl. Fusion 13, 509 (1973).

[4]D. A. Spong, J. F. Clarke, J. A. Rome, and T. Kammash, Nucl. Fusion 14, 397 (1974).

[5]J. D. Strachan and R. L. Dewar, in *Proceedings of the Fifth International Conference on Plasma Physics and Controlled Nuclear Fusion Research, Tokyo, Japan, 1974* (International Atomic Energy Agency, Vienna, 1975), Paper No. A8-1.

[6]B. Coppi, H. Knoepfel, and R. Pozzoli, Massachusetts Institute of Technology Plasma Research Report No. 745, 1974 (unpublished).

[7]S. von Goeler, W. Stodiek, N. Stauthoff, and H. Selberg, in *Proceedings of the Third International Symposium on Toroidal Plasma Confinement, Garching, Germany, 1973* (Max-Planck-Institut für Plasmaphysik, Garching, Germany, 1973).

[8]For example, M. J. Berger and S. M. Seltzer, Phys. Rev. C 2, 621 (1970); H. Ferdinande, G. Knyty, R. Van de Vijver, and R. Jacobs, Nucl. Instrum. Methods 91, 135 (1971).

[9]L. A. Berry *et al.*, in *Proceedings of the Fifth International Conference on Plasma Physics and Controlled Nuclear Fusion Research, Tokyo, Japan, 1974* (International Atomic Energy Agency, Vienna, 1975), Paper No. A5-1.

[10]P. Chrisman, J. F. Clarke, and J. A. Rome, ORNL Report No. ORNL-TM-4501, 1974 (unpublished).

[11]For example, J. A. Rome, J. D. Callen, and J. F. Clarke, Nucl. Fusion 14, 141 (1974).

[12]R. M. Kulsrud, Y. C. Sun, N. K. Winsor, and H. A. Fallon, Phys. Rev. Lett. 31, 690 (1973).